Hindawi
Advances in Polymer Technology
Volume 2022, Article ID 3206755, 12 pages
https://doi.org/10.1155/2022/3206755

Research Article

Electroresponsive Hydrogel-Based Switching Components for Soft, Bioelectrical, and Fluidic Circuits

Naner Li and Hemma Philamore

University of Bristol, Bristol BS8 1TH, UK

Correspondence should be addressed to Hemma Philamore; hemma.philamore@bristol.ac.uk

Received 15 November 2021; Revised 30 January 2022; Accepted 15 February 2022; Published 8 March 2022

Academic Editor: Wen Li

The development of various soft components for fluid circuits is conducive to the further development of soft robots. The electroresponsive hydrogel is applied to build a functional oscillator in the study conducted. Based on the multiphasic mixture model, the deformation of the hydrogel under external electric fields is analyzed through COMSOL Multiphysics simulator. Owing to the characteristics of the hydrogel that it will deform in response to electric field, the hydrogel is employed to control fluidic circuits, resulting in a novel controllable functional soft oscillator.

1. Introduction

Soft robot design is often inspired by creatures as they are mostly composed of soft components and they can move efficiently in their living environment. Compared to conventional robots, the softness of compliant materials makes soft robots more adaptive to the environment and more eco-friendly because most of the soft materials used to build soft robots, such as the hydrogel, are biodegradable. So, there is no need to recycle the robots when they are no longer functional in a remote environment. Moreover, soft robots show great safety superiority in human-robot interaction. Due to these advantages, researches on new applications of soft robotics have been popular, especially in medicine, wearable devices, environment monitoring, scientific exploration, disaster relief, and so on.

However, the flexibility and compliance of soft robots lead to low mechanical impedance, making them difficult to control. Many soft robots are built with a well-designed fluidic elastomer network which makes the robot deform or move in a conceived way as long as there is pneumatic or hydraulic input. Wehner et al. [1] developed an entirely soft octopus robot with two fluidic circuits, each of which controls a set of actuators of the octobot. In order to coordinate the movement of the two sets of actuators and realize the overall movement of the octobot, the researchers presented the oscillator of the soft controller to help the octobot alternate between two actuation states. However, the two actuation states are not independent and uncontrollable. In this case, it is necessary to design new switching components for the fluidic circuit to realize more advanced biomimetic, adaptive, and controllable behaviors of soft robots.

The control of most conventional robots is realized by electronic circuit, where various electronic devices, such as resistors, transistors, capacitors, inductors, and diodes, allow the electronic circuit to be able to modulate and convey the electric signal, further realizing the complex control of robots. However, in order to get rid of the rigid parts, soft robots apply fluidic circuits to replace electronic circuit. Hence, fluidic devices need to be developed correspondingly to control soft robots. In the research of Wehner et al. [1], the oscillator of octobot is the key component to control the movement of octobot, which is basically built by employing the switch valve proposed by Mosadegh et al. [2].

The main feature of smart hydrogels is their ability to respond to external stimuli, including temperature [3], pH [4], light [5], electric fields [6–8], and magnetic field [9, 10]. The electroresponsive hydrogel has huge potential to

Table 1: Overview of several applications of the hydrogel in fluidic devices.

Application	Schematic diagram	Hydrogel	Reference
Pump	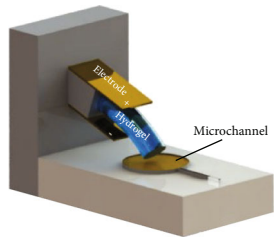	PAAm	[12]
Valve	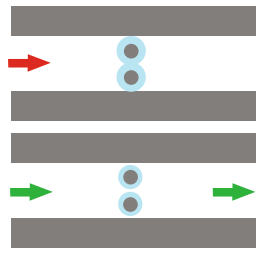	/	[13, 14]
Pressure valve		HEMA/AA	[15]
Check valve	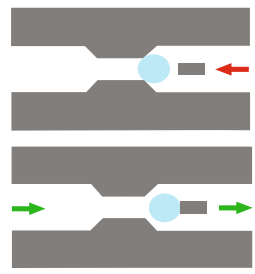	PEGDA	[16]
Flow sorter	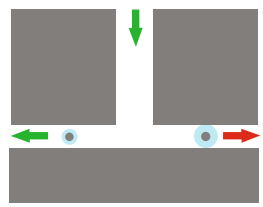	HEMA/AA HEMA/DMAEMA	[17]

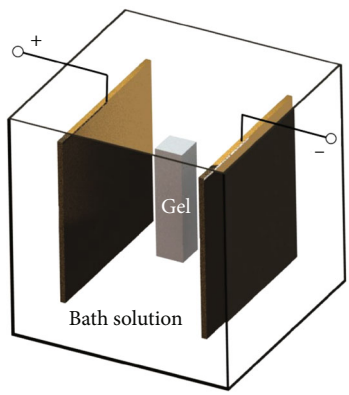

Figure 1: Ionic gel under external electric field.

be designed as a variety of fluidic devices as it can be controlled easily [11], and a few applications of the hydrogel are investigated and listed in Table 1. These existing researches show us the methods of developing different products based on the properties of the hydrogel, which will be the source of inspiration to develop new products by utilizing the hydrogel.

Although there are a number of researches about hydrogel-based fluidic devices, they mostly take advantage of the swelling properties of hydrogels to control the one-channel flow [13–16, 18–20]. However, researches on the hydrogel-based fluidic devices with different functions are not many, leaving us much room for study. In this study, the hydrogel is used to develop soft robotic switches, resulting in a novel functional oscillator.

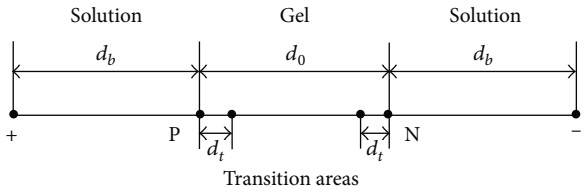

Figure 2: Computing model in one dimension.

2. Methods

Although the simulation software has been greatly advanced in recent years, there is still no module available to comprehensively describe hydrogel swelling, because the change of the hydrogel in response to external stimuli is a very complex process, involving osmotic pressure, rubber elasticity of the polymer network, and friction among phases [21]. In this case, we have to conduct a theoretical analysis for the hydrogel first to get control equations, and then the numerical model of the hydrogel can be constructed through partial differential equations in simulation software. Besides, the simulation of gel swelling faces many other challenges as follows:

(i) The changes of physical parameters are discontinuous at the interface of gel and solution

(ii) The interface of gel and solution will move as the gel swells

(iii) The geometric nonlinearity and material nonlinearity will occur when the deformation of gel is large

(iv) The calculation needs to couple multiphysics fields

Hence, the simulation of hydrogel-based oscillator is too complex to calculate and converge. In order to reduce the complexity of the simulation, we divided the simulation into two steps. In the first step, we analyzed the effect of external electric field on the hydrogel. We get to know the corresponding pressure on the gel under an external electric field with a given intensity. In the second step, we can apply the corresponding pressure instead of the external electric field. In other words, we only need to conduct a fluid-structure interaction study, in which the moving mesh is included to address the problem that the fluid domain reshapes due to the motion of the solid domain, to analyze the performance of hydrogel-based oscillator in the second step.

What should be noticed is that the gel researched in this study is ionic gel. Hydrogels can be classified in a number of ways. Depending on whether the groups on the polymer network can be ionized, the gel can be divided into neutral gel and ionic gel. Neutral gels only contain solvent and polymer network, whereas ionic gels contain free ions which affect the distribution of electric potential and serve as the key to response to the external electric field.

2.1. Deformation of Ionic Gel under External Electrical Field

2.1.1. Geometric Model. As is shown in Figure 1, a strip of gel is placed in the bath solution with electrodes at both ends. Assuming that the gel network has negative monovalent ions and the electrolyte in the solution is NaCl, the free cation and anion are Na+ and Cl-, respectively. If the deformation along the direction of gel thickness is considered merely, the problem above can be simplified as a one-dimensional problem as Figure 2 shows.

In Figure 2, + and - represent the positive and negative electrodes, respectively, and P and N are the interfaces of gel and solution near positive and negative electrodes, respectively. The region between P and N all belong to the gel, and the rest of region is the bath solution. What should be noticed here is that we add transition areas between gel and solution to reduce the nonlinearity of the physical parameters of the gel-solution interface. As this model is completely controlled by the control equations, there is no need to define the materials.

2.1.2. Dynamic Theory of Ionic Hydrogel Swelling. Collective diffusion model [22] and stress-diffusion coupled model [23] were raised for neutral gel, while transport model [24] was only applied to ionic gel. Meanwhile, multiphasic mixture model [25, 26] can be used to describe both neutral gel and ionic gel, considered as a universal and adaptable model. Hence, multiphasic mixture theory is applied to build the mathematical model. This modeling method is to disassemble porous medium into two or multiple phases. Each phase corresponds to a set of control equations, while there is coupling between these control equations.

(1) Constitutive Relation. The chemical or electrochemical potential of water μ_w and free ions μ_i can be calculated by

$$\mu_w = \mu_w^{\text{ref}} + \nu_w\left(p - RT\sum \Phi_i c_i\right), \tag{1}$$

$$\mu_i = \mu_i^{\text{ref}} + RT\ln\left(\gamma_i c_i\right) + Fz_i\psi, \tag{2}$$

where μ_w^{ref} and μ_i^{ref} are the reference chemical potential of water and free ions, respectively, ν_w is the molar volume of water molecule, p is the fluid pressure, R is the gas constant, c_i is the concentration of free ions, T is the ambient temperature, F is Faraday's constant, z_i is the valence electrons of free ions, and ψ is the electric potential inside gel. In addition, the subscripts "w," "i," "p," and "f" denote the water, free ions, polymer network, and fixed ions, respectively. If the concentration of free ions is relatively low, the osmotic coefficient Φ_i and activity coefficient γ_i of free ions are approximately equal to 1.

Assuming that the polymer network is isotropic, the elastic stress tensor of polymer network σ_p is expressed as

$$\sigma_p = \lambda \text{tr}(\varepsilon) I + 2\mu\varepsilon, \tag{3}$$

where λ and μ are the Lamé constants and ε is the strain

Table 2: The parameters for simulation.

Parameter	Value	Description
d_0	0.5 [cm]	Initial thickness of gel
d_b	0.5 [cm]	The width of bath solution on both sides
d_t	0.04 [cm]	The width of transition area
F	9.648×104 [C/mol]	Faraday's constant
R	8.314 [J/(mol•K)]	Gas constant
ε_0	$8.854 \times 10 - 12$ [C^2/(N•m^2)]	Vacuum permittivity
ε	80	Relative permittivity
z_+	+1	Valence electrons of cation
z_-	-1	Valence electrons of anion
z_f	-1	Valence electrons of fixed ion
λ	1.44×105 [Pa]	The first Lamé constants
μ	8×103 [Pa]	The second Lamé constants
D_i	$1.0 \times 10 - 7$ [m^2/s]	Diffusion coefficient
f_{wp}	5.0×1012 [N•s/m^4]	Friction coefficient between water and gel network
ϕ_{w0}	0.8	Initial volume fraction of water in the gel
T	298 [K]	Ambient temperature
c_0	1 [mol/m^3]	Initial concentration of free ions
c_{f0}	5 [mol/m^3]	Initial concentration of fixed ions
ψ_0	0.15 [V]	Electric potential at the electrode

stress that can be calculated by

$$\varepsilon_{ij} = \frac{1}{2}\left(\frac{\partial u_i}{\partial x_j} + \frac{\partial u_j}{\partial x_i}\right). \tag{4}$$

When the gel deforms, the volume fraction of water in the gel will change. The relation between the volume fraction and strain can be expressed as

$$\varphi_w = \frac{\varphi_{w0} + \mathrm{tr}(\varepsilon)}{1 + \mathrm{tr}(\varepsilon)}, \tag{5}$$

where ϕ_{w0} is the initial volume fraction of water in the gel, and the further relationship between the volume fraction and the concentration of fixed ions can be expressed as

$$c_f = c_{f0}\frac{\varphi_{w0}(1-\varphi_w)}{\varphi_w(1-\varphi_{w0})} = c_{f0}\frac{\varphi_{w0}}{\varphi_{w0} + \mathrm{tr}(\varepsilon)}, \tag{6}$$

where c_{f0} is the initial concentration of fixed ions.

(2) Mass Conservation. The mass conservation equations of polymer network, water, and free ions in the gel are

$$\begin{cases} \dfrac{\partial \varphi_p}{\partial t} + \nabla\left(\varphi_p v_p\right) = 0, \\ \dfrac{\partial \varphi_w}{\partial t} + \nabla(\varphi_w v_w) = 0, \\ \dfrac{\partial(\varphi_w c_i)}{\partial t} + \nabla(\varphi_w c_i v_w) = 0 \ (i = +,-). \end{cases} \tag{7}$$

Assume that the gel only consists of three phases: polymer network, water, and free ions. However, the volume fraction of free ions is usually relatively low compared to the volume fraction of polymer network and water, so we have

$$\varphi_p + \varphi_w + \sum \varphi_i = 1. \tag{8}$$

Integrating equation (7), we can derive

$$\nabla \cdot \left(\varphi_w v_w + \varphi_p v_p\right) = 0. \tag{9}$$

Substituting equations (8) to (9), we have

$$\nabla \cdot v_p = \nabla \cdot \left(\varphi_w\left(v_p - v_w\right)\right). \tag{10}$$

(3) Momentum Conservation. (i) Momentum conservation of polymer network.

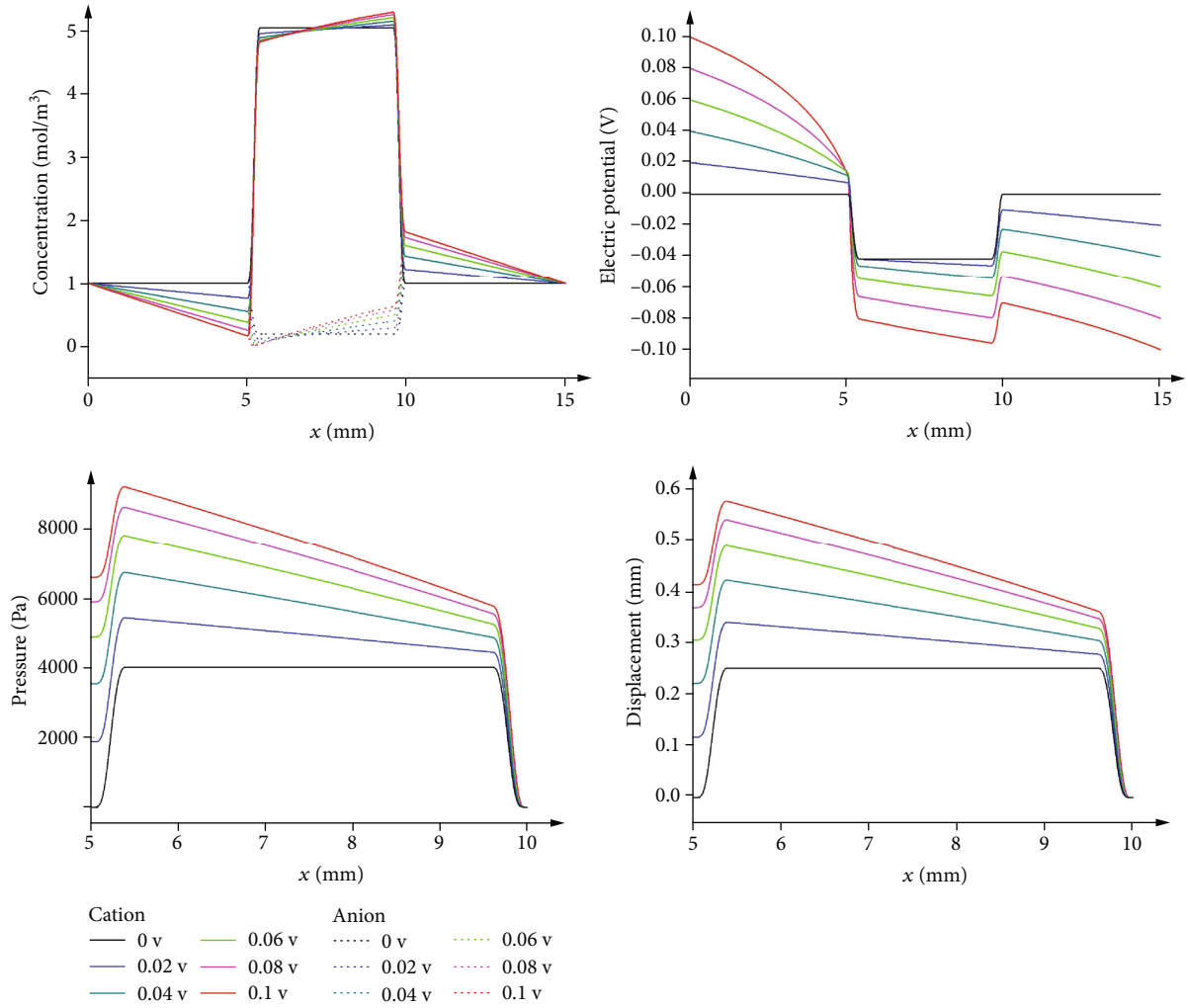

Figure 3: The distribution of free ion concentration, electric potential, fluid pressure, and displacement under different external electric field.

$$\nabla \cdot \sigma_p - \varphi_w z_f c_f F \nabla \psi - \varphi_p \nabla p + f_{pw}(v_w - v_p) = 0, \quad (11)$$

where the first term of formula represents the divergence of the elastic stress tensor of the polymer network, the second term corresponds to the electrostatic force, the third term comes from the osmotic pressure difference, and the last term is the friction between the polymer network and water, in which f_{pw} denotes the coefficient of friction between phase polymer network and water.

(ii) Momentum Conservation of Water

The driving force of water comes from the contribution of the chemical potential gradient of water and the friction between phases, while the viscous resistance and the inertial force are neglected.

$$-\frac{\varphi_w}{v_w}\nabla \mu_w + f_{wp}(v_p - v_w) + \sum_{i=+,-} f_{wi}(v_i - v_w) = 0. \quad (12)$$

Substituting equation (1) to (12), we have

$$-\varphi_w\left(\nabla p - RT\sum \nabla c_i\right) + f_{wp}(v_p - v_w) + \sum_{i=+,-} f_{wi}(v_i - v_w) = 0. \quad (13)$$

(iii) Momentum conservation of free ions

Similar to water, free ions are driven by the chemical potential gradient, while the inertial force and the resistance from the collision among free ions are neglected.

$$-\varphi_w(RT\nabla c_i + Fz_i c_i \nabla \psi) + f_{wi}(v_w - v_i) = 0. \quad (14)$$

(4) Control Equation. Define the flux of free ions as

$$J_i = \varphi_w c_i v_i. \quad (15)$$

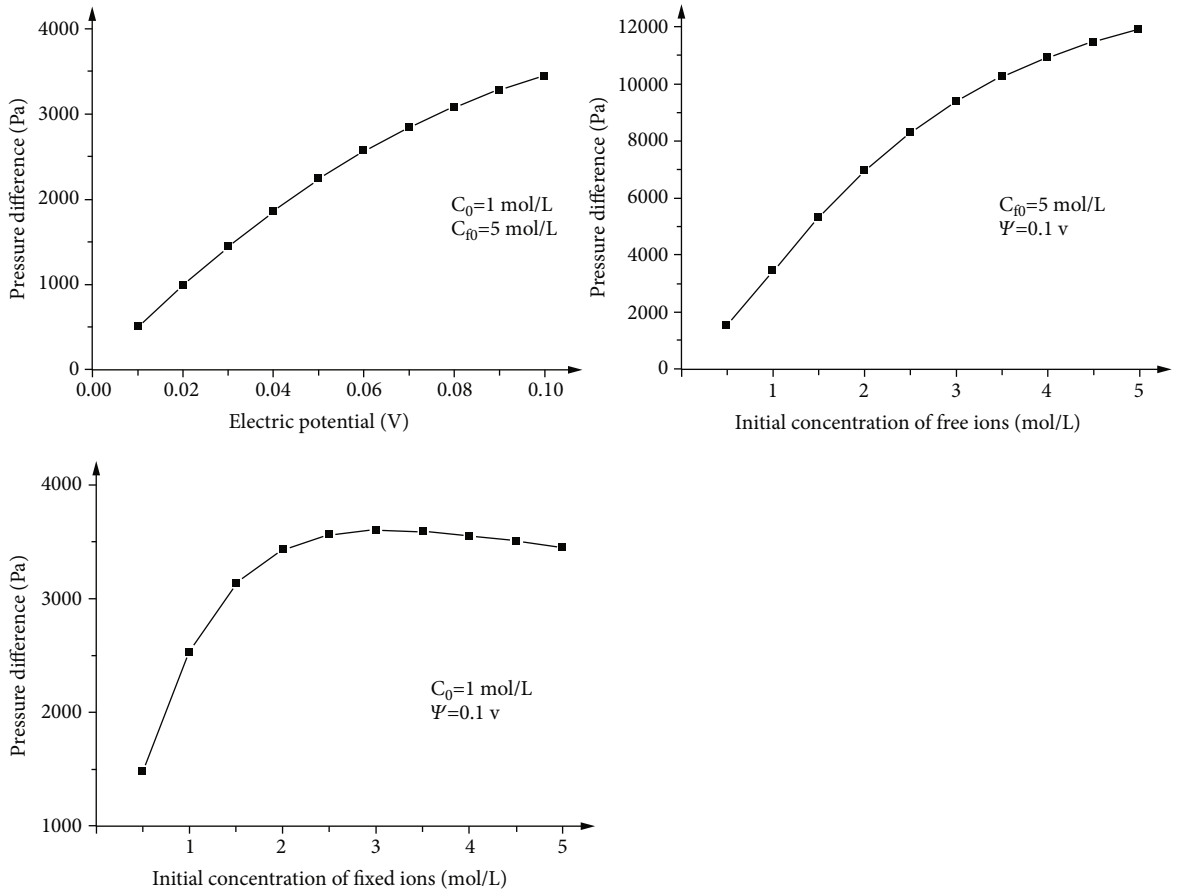

Figure 4: The effects of electric potential, free ion concentration, and fixed ion concentration on the pressure difference.

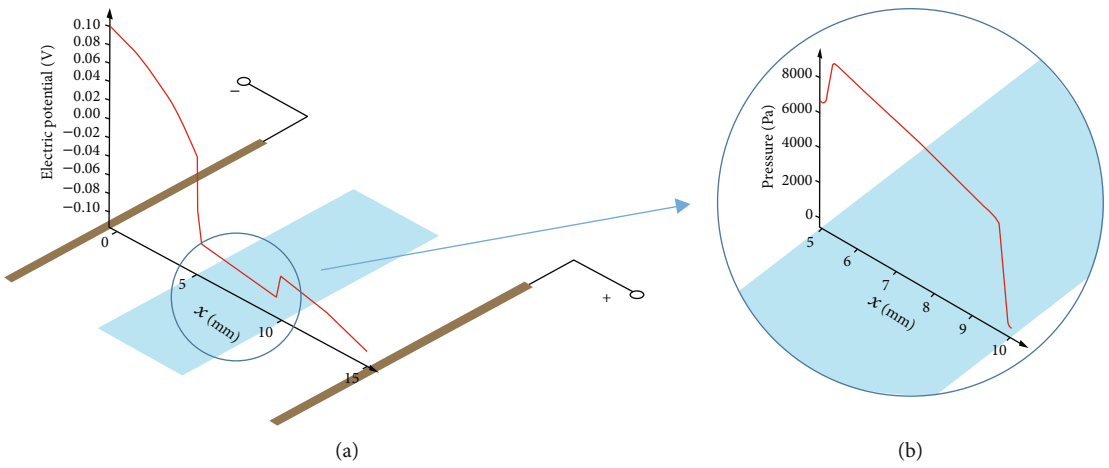

Figure 5: (a) The electric potential distribution of the hydrogel under an external electric field. (b) The corresponding pressure distribution of the hydrogel.

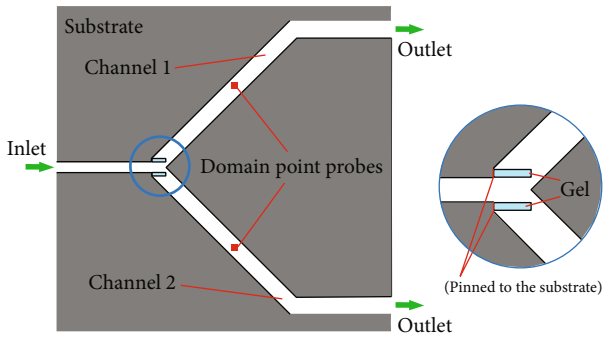

Figure 6: Oscillator computing model in COMSOL Multiphysics.

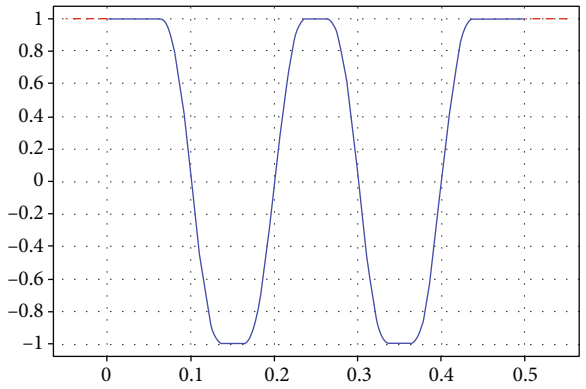

Figure 7: A unit piecewise function showing the same curve of input signal.

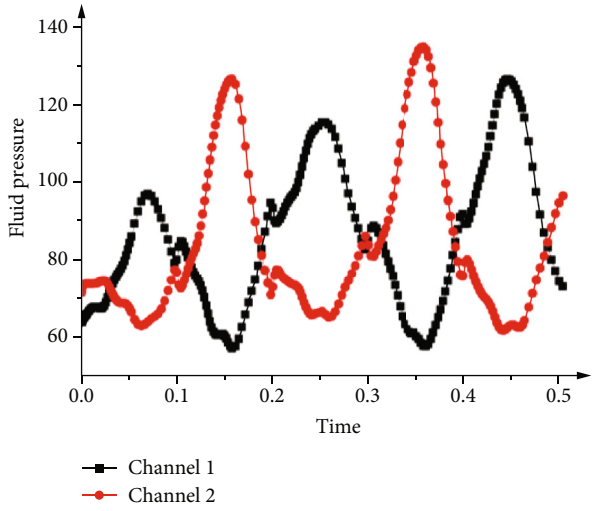

Figure 8: Fluid pressure change of two channels.

Substituting equation (14) to (15), we have

$$J_i = -\frac{RT}{f_{wi}}\varphi_w^2 c_i \nabla c_i - \frac{Fz_i}{f_{wi}}\varphi_w^2 c_i^2 \nabla\psi + \varphi_w c_i v_w, \tag{16}$$

where the last term of formula represents the convective diffusion generated by the water flow. However, gel swelling is such a slow process that the contribution of convection-diffusion to free ion flux can be ignored. Meanwhile, the diffusion coefficient of free ions is introduced:

$$D_i = \frac{RT}{f_{wi}}\varphi_w c_i. \tag{17}$$

Then, we have

$$J_i = -\varphi_w D_i\left(\nabla c_i + \frac{Fz_i}{RT}c_i\nabla\psi\right). \tag{18}$$

Then, we can derive all control equations for ionic hydrogel multiphase model as follows. Substituting equation (18) to (7), we have

$$\frac{\partial(\varphi_w c_i)}{\partial t} = D_i\nabla\left(\varphi_w\left(\nabla c_i + \frac{Fz_i}{RT}c_i\nabla\psi\right)\right). \tag{19}$$

Usually, the size of the studied gel sample is much larger than the Debye length, so it can be said that the electric neutral condition is met inside the gel. In this case, adding (11), (13), and (14) together, then we have

$$\nabla\cdot\left(\sigma_p - pI\right) = 0. \tag{20}$$

Substituting (13) and (14) to (10), we have

$$\nabla\cdot v_p = \nabla\cdot\left(\frac{\varphi_w^2}{f_{wp}}\left(\nabla p + F\nabla\psi\sum z_i c_i\right)\right). \tag{21}$$

To couple the concentration and potential of free ions, Poisson's equation is applied:

$$\nabla^2\psi = -\frac{F}{\varepsilon\varepsilon_0}\varphi_w\left(z_f c_f + \sum z_i c_i\right). \tag{22}$$

These four control equations involve four independent unknown variables: the displacement of polymer network, the pressure of fluid, the concentration of free ions, and the electric potential. Hence, we need to set boundary conditions of c_i and ψ at electrodes and boundary conditions of p and μ at the gel-solution interfaces.

$$\begin{cases} c_i|_+ = c_i|_- = c_0, \\ \psi|_+ = \psi_0, \\ \psi|_- = -\psi_0, \\ p|_P = 0, \\ p|_N = (\lambda + 2\mu)\nabla u. \end{cases} \tag{23}$$

The parameters occurred are specified in Table 2.

2.1.3. Result. In COMSOL Multiphysics, users can conduct the coupling analysis of arbitrary physical fields. For this study, what is on top of the agenda is a coupling analysis of four physical fields, including displacement field, pressure

Table 3: Pressure change over a period.

Time	Pressure distribution of fluid domain	Pressure distribution of solid domain
T/10		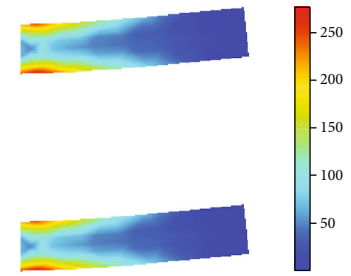
2T/10	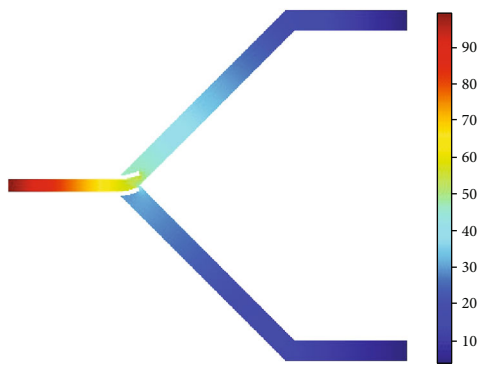	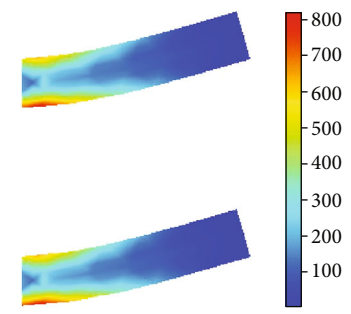
3T/10	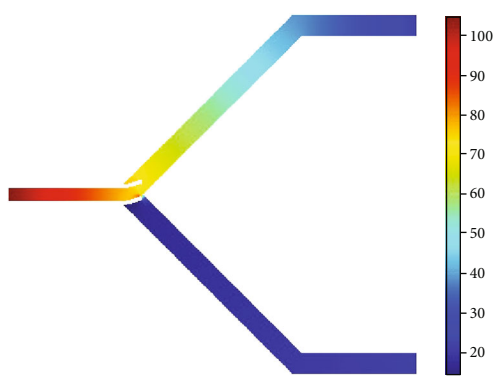	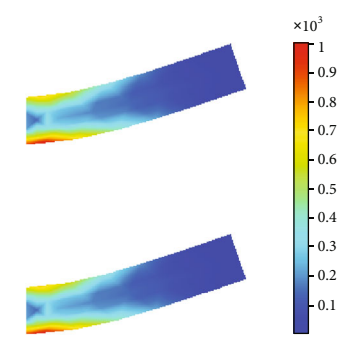
4T/10	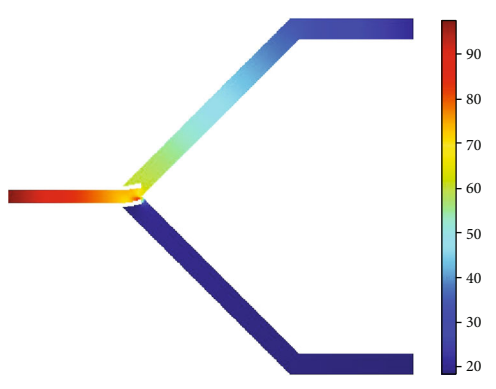	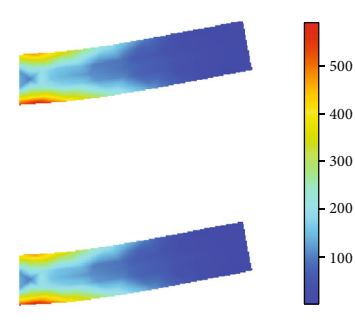

Table 3: Continued.

Time	Pressure distribution of fluid domain	Pressure distribution of solid domain
5T/10		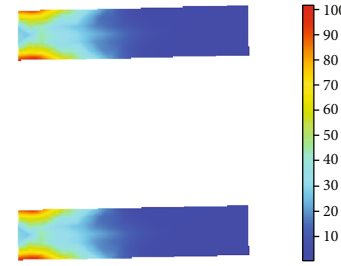
6T/10		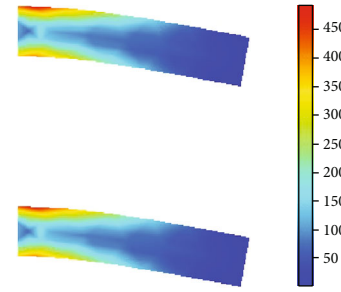
7T/10		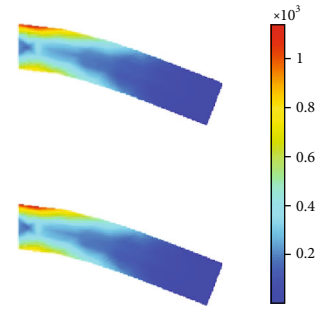
8T/10		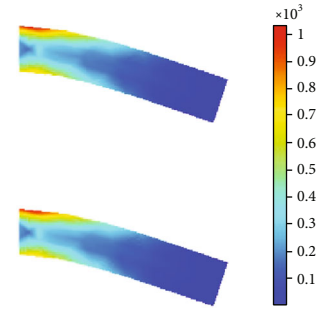

Table 3: Continued.

Time	Pressure distribution of fluid domain	Pressure distribution of solid domain
9T/10	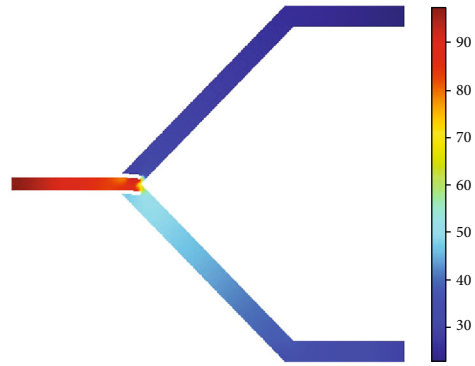	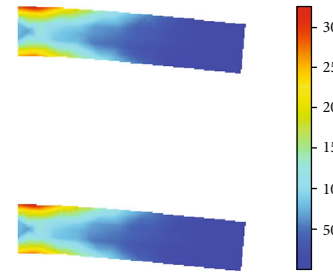
T	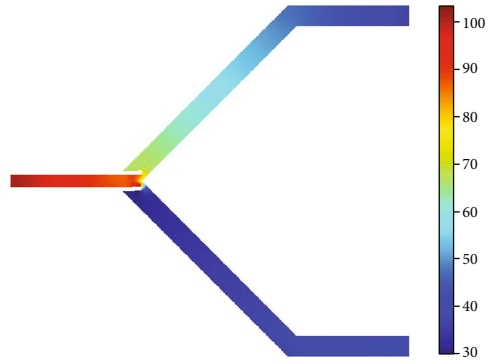	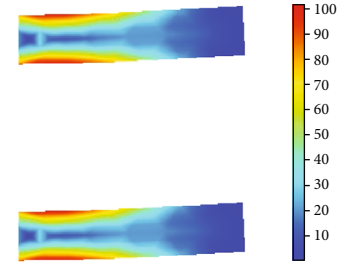

field, concentration field, and electric field. Through the PDE module, the control equations can be used to build the multiphysical field coupling model. With the boundary conditions set above, the model can be solved accordingly.

Figure 3 shows the distribution of free ion concentration, electric potential, fluid pressure and displacement under a series of different electric fields, where the x axis can be seen as the one-dimension model and the y axis shows values at each point of model. As can be seen from Figure 3, after applying the electric field, the distribution of each physical quantity in the gel and bath solution is no longer uniform. The concentrations of free cations and anions increase near the negative electrode and decrease near the positive electrode, overlapping in the bath solution while there is a big gap in the gel as most cations in the gel are ionized from the fixed groups. As the electric potential increases, the fluid pressure in the gel gradually increases. Obviously, the nonuniformity of electric potential distribution in the gel is triggered by the nonuniformity of free ion concentration distribution, resulting in the nonuniform distribution of pressure. The pressure difference between the two sides of gel is the reason why ionic hydrogels with fixed anions bend towards the negative electrode in an external electric field.

Hence, we can define the pressure difference between the two sides of gel Δp to indicate the influence of the applied electric field on the equilibrium swelling state of ionic hydrogel.

$$\Delta p = p|_{\text{Left}} - p|_{\text{Right}}, \tag{24}$$

where the bigger value of Δp represents the larger bending degree of ionic hydrogel in the applied electric field and the sign of Δp indicates the direction of bending. The positive sign and negative sign represent the gel bend to the negative electrode and positive electrode, respectively.

Figure 4 shows the effects of electric potential, free ion concentration, and fixed ion concentration on Δp. From Figure 4, we can see that Δp gets larger as the electric potential or free ion concentration increases. However, the rising tendency of Δp gradually slows down as the electric potential or free ion concentration increases. With the increase of fixed ion concentration, Δp increases rapidly first, reaches the peak at 3 mol/L, and then decreases slowly and steadily.

2.2. Peformence of Gel-Based Oscillator. In the last section, we analyzed the effect of external electric field on the hydrogel. We can know the corresponding pressure on the gel under an external electric field with a given intensity. So in this section, we can apply the corresponding pressure instead of the external electric field, as is shown in Figure 5.

Figure 6 shows the model of an oscillator. The liquid filling the channels is water, and we set constant pressure of 100 Pa at fluid inlet and 0 Pa at fluid outlet. One thing that should be mentioned is we only analyzed the hydrogel oscillator qualitatively but not quantitatively, as the value of oscillation signal partly depends on the fluid domain material and input pressure which can be manually set and the goal of this study is to verify the feasibility of hydrogel oscillator. The analysis is not aimed at a specific system, so the values shown in the figures are not strictly meaningful.

A unit piecewise function shown in Figure 7 is employed to help set the input signal, which will be multiplied by the value of corresponding pressure. Then, we collect the data from two domain point probes in two channels to demonstrate the pressure change of two channels, as is shown in Figure 8. From Figure 8, we can see that the hydrogel oscillator successfully oscillates the pressure in two channels. Although there are some noises, we can clearly see that the pressure peaks appear alternately in the two channels.

Table 3 visually shows the pressure change over a period T. In the initial phase, at T/10, the gel does not respond immediately to the input signal, so the pressure distribution is nearly the same in both channels. From 2T/10 to 4T/10, the gel bends to channel 1, blocking the flow to channel 2. Naturally, the pressure in channel 1 builds up and the pressure in channel 2 drops, which can also be seen in Figure 7. At 5T/10, the gel returns, as well as the pressure of two channels, to the central point. In the last half period, the gel bends to channel 2. Similarly, the pressure in channel 2 builds up and the pressure in channel 1 drops.

3. Conclusion

Based on the multiphasic mixture theory of gel swelling, on the finite element software platform COMSOL Multiphysics, this study simulated the swelling of ionic hydrogel under an applied electric field and numerically analyzed the influence of related environmental parameters and material parameters on the equilibrium state of gel swelling. The numerical simulation results confirm the response of ionic hydrogels to the applied electric field, and the hydrogels with negative valence ions will bend towards the negative electrode. Meanwhile, the initial concentration of the fixed ions on the polymer network, the concentration of the surrounding solution, and the intensity of the applied external electric field will affect the swelling equilibrium state of the gel.

Based on the research findings of ionic hydrogel, COMSOL Multiphysics was used to simulate the response of ionic hydrogel to input signal and its influence on the fluidic circuits. It turns out that the hydrogel can control the flow path by deformation, which verifies the feasibility of hydrogel-based oscillator. With a specific signal input, the hydrogel can become a controllable functional soft oscillator. In three-dimensional space, the hydrogel oscillator has the potential to control more than two flow channels.

Data Availability

The data used to support the findings of this study are available from the corresponding author upon request.

Conflicts of Interest

The authors declare that they have no conflicts of interest.

References

[1] M. Wehner, R. L. Truby, D. J. Fitzgerald et al., "An integrated design and fabrication strategy for entirely soft, autonomous robots," *Nature*, vol. 536, no. 7617, pp. 451–455, 2016.

[2] B. Mosadegh, C. H. Kuo, Y. C. Tung et al., "Integrated elastomeric components for autonomous regulation of sequential and oscillatory flow switching in microfluidic devices," *Nature Physics*, vol. 6, no. 6, pp. 433–437, 2010.

[3] J. Hu, N. Jiang, and J. Du, "Thermally controlled large deformation in temperature-sensitive hydrogels bilayers," *International Journal of Smart and Nano Materials*, vol. 12, no. 4, pp. 450–471, 2021.

[4] H. Haidari, Z. Kopecki, A. T. Sutton, S. Garg, A. J. Cowin, and K. Vasilev, "pH-responsive "Smart" hydrogel for controlled delivery of silver nanoparticles to infected wounds," *Antibiotics*, vol. 10, no. 1, p. 49, 2021.

[5] X. S. Lin, W. W. Xie, Q. Lin et al., "NIR-responsive metal-containing polymer hydrogel for light-controlled microvalve," *Polymer Chemistry*, vol. 12, no. 23, pp. 3375–3382, 2021.

[6] Y. Shin, M. Y. Choi, J. Choi, J. H. Na, and S. Y. Kim, "Design of an electro-stimulated hydrogel actuator system with fast flexible folding deformation under a low electric field," *ACS Applied Materials & Interfaces*, vol. 13, no. 13, pp. 15633–15646, 2021.

[7] H. Y. Jiang and J. G. Tang, "Zirconium hydroxide cross-linked nanocomposite hydrogel with high mechanical strength and fast electro-response," *ACS Applied Polymer Materials*, vol. 2, no. 9, pp. 3821–3827, 2020.

[8] P. Jaruchalermrat and S. Niamlang, "Development of cornstarch-based hydrogel drug delivery patch controlled by the electric field for hypertension," *Journal of Physics: Conference Series*, vol. 1719, no. 1, p. 012074, 2021.

[9] A. V. Shibaev, M. E. Smirnova, D. E. Kessel, S. A. Bedin, I. V. Razumovskaya, and O. E. Philippova, "Remotely self-healable, shapeable and pH-sensitive dual cross-linked polysaccharide hydrogels with fast response to magnetic field," *Nanomaterials*, vol. 11, no. 5, p. 1271, 2021.

[10] Z. Y. Jia, M. Müller, T. L. Gall et al., "Multiplexed detection and differentiation of bacterial enzymes and bacteria by color-encoded sensor hydrogels," *Bioactive Materials*, vol. 6, no. 12, pp. 4286–4300, 2021.

[11] R. X. Li, X. Z. Zhang, J. S. Zhao, J. M. Wu, Y. Guo, and J. Guan, "Preparation and electroresponsive property of poly (vinyl alcohol)/sodium alginate composite hydrogel," *Journal of Applied Polymer Science*, vol. 101, no. 5, pp. 3493–3496, 2006.

[12] E. A. Moschou, S. F. Peteu, L. G. Bachas, M. J. Madou, and S. Daunert, "Artificial muscle material with fast electroactuation under neutral pH conditions," *Chemistry of Materials*, vol. 16, no. 12, pp. 2499–2502, 2004.

[13] N. Arbabi, M. Baghani, J. Abdolahi, H. Mazaheri, and M. Mosavi-Mashhadi, "Study on pH-sensitive hydrogel micro-valves: a fluid–structure interaction approach," *Journal of Intelligent Material Systems and Structures*, vol. 28, no. 12, pp. 1589–1602, 2017.

[14] Z. S. Liu, W. Toh, and T. Y. Ng, "Advances in mechanics of soft materials: a review of large deformation behavior of hydrogels," *International Journal of Applied Mechanics*, vol. 7, no. 5, article 1530001, 2015.

[15] R. H. Liu, Q. Yu, and D. J. Beebe, "Fabrication and characterization of hydrogel-based microvalves," *Journal of Microelectromechanical Systems*, vol. 11, no. 1, pp. 45–53, 2002.

[16] Y. Z. Wang, K. Toyoda, K. Uesugi, and K. Morishima, "A simple micro check valve using a photo-patterned hydrogel valve core," *Sensors and Actuators, A: Physical*, vol. 304, article 111878, 2020.

[17] E. Khanjani, A. Hajarian, A. Kargar-Estahbanaty, N. Arbabi, A. Taheri, and M. Baghani, "Design and fluid-structure interaction analysis for a microfluidic T-junction with chemo-responsive hydrogel valves," *Applied Mathematics and Mechanics*, vol. 41, no. 6, pp. 939–952, 2020.

[18] A. Ghasemkhani and H. Mazaheri, "Study of functionally graded temperature-sensitive hydrogel micro-valve considering fluid-structure interactions," *Modares Mechanical Engineering*, vol. 20, pp. 943–951, 2020.

[19] H. Mazaheri, A. H. Namdar, and A. Amir, "Behavior of a smart one-way micro-valve considering fluid–structure interaction," *Journal of Intelligent Material Systems and Structures*, vol. 29, no. 20, pp. 3960–3971, 2018.

[20] P. J. Mehner, M. Allerdißen, S. Haefner, A. Voigt, U. Marschner, and A. Richter, "Modeling the closing behavior of a smart hydrogel micro-valve," *Journal of Intelligent Material Systems and Structures*, vol. 30, no. 9, pp. 1409–1418, 2019.

[21] T. Tanaka, I. Nishio, S. T. Sun, and S. Ueno-Nishio, "Collapse of gels in an electric field," *Science*, vol. 218, no. 4571, pp. 467–469, 1982.

[22] Y. Li and T. Tanaka, "Kinetics of swelling and shrinking of gels," *The Journal of Chemical Physics*, vol. 92, no. 2, pp. 1365–1371, 1990.

[23] T. Yamaue and M. Doi, "The stress diffusion coupling in the swelling dynamics of cylindrical gels," *The Journal of Chemical Physics*, vol. 122, no. 8, p. 084703, 2005.

[24] S. N. Wu, H. Li, J. P. Chen, and K. Y. Lam, "Modeling investigation of hydrogel volume transition," *Macromolecular Theory and Simulations*, vol. 13, no. 1, pp. 13–29, 2004.

[25] Y. Guang, A. J. Cocciolone, C. L. Crandall, B. B. Johnston, L. A. Setton, and J. E. Wagenseil, "A multiphasic model for determination of water and solute transport across the arterial wall: effects of elastic fiber defects," *Archive of Applied Mechanics*, vol. 91, no. 6, pp. 1–13, 2021.

[26] H. Li, X. Wang, Z. Wang, and K. Y. Lam, "Multiphysics modelling of volume phase transition of ionic hydrogels responsive to thermal stimulus," *Macromolecular Bioscience*, vol. 5, no. 9, pp. 904–914, 2005.